A Stable Mercury-Containing Complex of the Organomercurial Lyase MerB: Catalysis, Product Release, and Direct Transfer to MerA†

Gregory C. Benison,‡ Paola Di Lello,§ Jacob E. Shokes,‡ Nathaniel J. Cosper,‡,|| Robert A. Scott,‡,§,|| Pascale Legault,*,§ and James G. Omichinski*,‡,§

Department of Chemistry, Department of Biochemistry and Molecular Biology, and Center for Metalloenzyme Studies, University of Georgia, Athens, Georgia 30602

Received February 13, 2004; Revised Manuscript Received May 4, 2004

ABSTRACT: Bacteria isolated from organic mercury-contaminated sites have developed a system of two enzymes that allows them to efficiently convert both ionic and organic mercury compounds to the less toxic elemental mercury. Both enzymes are encoded on the *mer* operon and require sulfhydryl-bound substrates. The first enzyme is an organomercurial lyase (MerB), and the second enzyme is a mercuric ion reductase (MerA). MerB catalyzes the protonolysis of the carbon−mercury bond, resulting in the formation of a reduced carbon compound and inorganic ionic mercury. Of several mercury-containing MerB complexes that we attempted to prepare, the most stable was a complex consisting of the organomercurial lyase (MerB), a mercuric ion, and a molecule of the MerB inhibitor dithiothreitol (DTT). Nuclear magnetic resonance (NMR) spectroscopy and extended X-ray absorption fine structure spectroscopy of the MerB/Hg/DTT complex have shown that the ligands to the mercuric ion in the complex consist of both sulfurs from the DTT molecule and one cysteine ligand, C96, from the protein. The stability of the MerB/Hg/DTT complex, even in the presence of a large excess of competing cysteine, has been demonstrated by NMR and dialysis. We used an enzyme buffering test to determine that the MerB/Hg/DTT complex acts as a substrate for the mercuric reductase MerA. The observed MerA activity is higher than the expected activity assuming free diffusion of the mercuric ion from MerB to MerA. This suggests that the mercuric ion can be transferred between the two enzymes by a direct transfer mechanism.

Mercury compounds, especially organomercurial compounds such as methylmercury (MeHg), have been responsible for a significant amount of human poisoning and environmental degradation (*1*). Mercury and its compounds are introduced into the environment by both natural and anthropogenic processes (*2*, *3*). Although the highly toxic compound MeHg has been introduced into the environment directly by industrial processes, this compound can also be produced from less toxic forms of mercury by bacteria in aquatic sediments (*4*, *5*). MeHg can appear in humans, fish, and other animals in high concentrations because of its tendency to biomagnify (*2*, *6*). These concerns have led to regulation of the uses of mercury as well as efforts to clean up mercury pollution (*7*).

A variety of methods for the remediation of mercury pollution are proposed or in use (*8*). Some methods involve physical removal or decontamination of soil or water. An alternative is to use the naturally occurring mercury-detoxifying capability of certain bacterial strains in bioremediation schemes. Bioremediation schemes have been developed using the microorganisms themselves (*9*) or by incorporating the bacterial mercury resistance genes into plants (*10*, *11*). The method of using plants to remediate pollution, known as phytoremediation, has several desirable properties: plants have a large biomass, can grow in many of the polluted habitats, and are inexpensive (*12*, *13*).

Mercury resistant bacterial strains possess a set of genes known as the *mer* operon, which is usually found on plasmids (*14*). These genes allow resistant strains to thrive in the presence of ionic or organic mercury compounds that are highly toxic to nonresistant bacteria or other forms of life. Ionic mercury is detoxified by a series of transport steps culminating in reduction by MerA to elemental mercury [Hg(0)]. Transport begins when ionic mercury [Hg(II)] is bound to MerP in the periplasm. Hg(II) is then transferred to the membrane protein MerT and from there to the enzyme mercuric reductase (MerA) in the cytosol. MerA reduces the mercuric ion to elemental mercury. It has been proposed that the transfer of Hg(II) both from MerP to MerT and from

† G.C.B. was funded by a National Science Foundation Graduate Research Fellowship. This work was supported by American Cancer Society Grant RPG LBC-100183 (J.G.O.). XAS work in the laboratory of R.A.S. is supported by the National Institutes of Health (GM 42025). Portions of this research were carried out at the Stanford Synchrotron Radiation Laboratory (SSRL), a national user facility operated by Stanford University on behalf of the U.S. Department of Energy, Office of Basic Energy Sciences. The SSRL Structural Molecular Biology Program is supported by the Department of Energy, Office of Biological and Environmental Research, and by the National Institutes of Health, National Center for Research Resources, Biomedical Technology Program.

* To whom correspondence should be addressed. Current address: Université de Montréal, Département de Biochimie, C. P. 6128, Succ. Centreville, Montréal, Quebec H3C 3J7, Canada. Tel: 514-343-7341. Fax: 514-343-2210. E-mail (J.G.O.): jg.omichinski@umontreal.ca. E-mail (P.L.): pascale.legault@umontreal.ca.

‡ Department of Chemistry.

§ Department of Biochemistry and Molecular Biology.

|| Center for Metalloenzyme Studies.

10.1021/bi049662h CCC: $27.50
Published on Web 06/12/2004

MerT to MerA can occur by a direct protein-to-protein transfer mechanism (*15*). Organomercurials, because of their hydrophobicity, can enter the cytosol without the use of such a transport mechanism. Once in the cytosol, organomercurials are cleaved by the enzyme organomercurial lyase (MerB), yielding a mercuric ion and the reduced organic product. Then, MerA reduces the mercuric ion to a mercury atom. The elemental mercury atom produced by either process is less toxic than either the organic mercury compound or the mercuric ion, and it can also easily leave the cell due to its volatility.

MerB accepts a very wide variety of organomercurial substrates (*16*). MerB also requires a thiol cofactor for turnover in vitro. Many single sulfhydryl-containing thiol compounds, including cysteine, glutathione, and β-mercaptoethanol, are suitable, whereas the two sulfur-containing compound DTT[1] is highly inhibiting (*16*, *17*). There are many known *merB* genes from a variety of microorganisms. Most of the *merB* genes are very homologous to each other but lack homology to any known non-*merB* prokaryotic or eukaryotic genes (*17*). The biochemical challenge that MerB must meet is to bind a variety of organomercurial compounds tightly enough to be an effective catalyst, yet release the product mercuric ion at a useful rate (*18*).

MerA must meet a similar biochemical challenge: it must compete effectively for mercuric ions with other tightly bound thiol ligands; yet, it must not bind the mercuric ion so tightly that reduction and turnover are not possible (*18*, *19*). MerA is a flavoprotein similar in structure and sequence to other disulfide oxidoreductases (*20*). The reduction of the mercuric ion is mediated by a pair of redox active cysteines near the FAD binding site. One major structural feature found in MerA and not in related proteins is a ~15 residue carboxyl-terminal extension containing two additional, adjacent cysteine residues. These carboxyl-terminal cysteine residues are essential for catalytic turnover both in vitro and in vivo (*21*). The function of the carboxyl-terminal cysteines is to remove thiol ligands from the mercuric ion substrate (*22*). MerA also possesses an amino-terminal domain not found in homologous disulfide oxidoreductases. The amino-terminal domain of MerA is homologous to MerP and contains two conserved cysteine residues. Early experiments showed that removal of these two cysteines does not affect the catalytic turnover rate in vitro (*21*). However, it has more recently been shown that a complex of the amino-terminal domain and a mercuric ion can serve as a substrate for the catalytic core (*15*). This finding suggests that the amino-terminal domain may actually have an important function in vivo.

To further understand catalysis by the unique enzyme MerB, we have explored several avenues for the preparation of mercury-containing MerB complexes. The most stable and reproducible complex prepared consisted of MerB, one mercuric ion, and a molecule of DTT. Mercury coordination in the MerB/Hg/DTT complex was characterized by extended X-ray absorption fine structure spectroscopy (EXAFS) and NMR spectroscopy. We have determined the stability of the MerB/Hg/DTT complex under a variety of thiol conditions. Because it has been suggested that product release from MerB occurs via a direct transfer mechanism, in which the mercuric ion passes directly from the active site of MerB to the active site of MerA without first diffusing through the cytoplasm (*23*), we have also tested this hypothesis using the MerB/Hg/DTT complex as a substrate for MerA in a kinetic assay.

MATERIALS AND METHODS

MerB Purification. The *merB* gene from plasmid R831b (*24*) was amplified by polymerase chain reaction, and the *NdeI*/*XhoI* fragment was ligated into the expression vector pET21b (Novagen). The resulting plasmid was identical to pQZB1 (*17*) except for the insertion of a stop codon between the *XhoI* site and the MerB-encoding sequence. This construct prevented the expression of the histidine tag present in pET21b.

The protein was purified from BL21(DE3) cells containing the MerB-encoding plasmid. Unlabeled protein was produced by growing cells in Luria−Bertani (LB) broth at 37 °C for 24 h. Uniform (>98% ^{15}N-labeled MerB protein was produced by growing cells in modified minimal medium containing ^{15}N-labeled NH_4Cl as the sole nitrogen source and with continual induction by 10−20 μM isopropyl D-thiogalactoside (IPTG). In LB broth, there was sufficient expression without any induction by IPTG. All media contained 0.1 mg/mL ampicillin to retain the plasmid.

Purification was based on the scheme of Begley et al. (*25*). All steps were performed at 4 °C, and DTT-containing solutions were freshly prepared before use. The cells from 3 L of culture were harvested by centrifugation in a Beckman JA-10 rotor at 5000*g* for 20 min and then suspended in 150 mL of buffer A [20 mM Tris (pH 8.0), 1 mM DTT, and 1 mM EDTA] plus 1 mg/mL benzamidine. The suspension was passed through a French press and centrifuged at 100000*g* for 1 h. The supernatant was applied to a DEAE-sepharose Fast Flow (Amersham Biosciences) column (50 mm i.d. × 40 cm length) equilibrated with buffer A, and MerB was eluted with a salt gradient of 0−1 M NaCl over 1.5 L. MerB-containing fractions were identified by polyacrylamide gel electrophoresis, pooled, dialyzed with a 10K ultrafiltration membrane (Millipore) into buffer B [20 mM sodium phosphate (pH 7.2), 1 mM EDTA, and 1 mM DTT], applied to a Q-sepharose Fast Flow (Amersham Biosciences) column (26 mm i.d. × 40 cm length) equilibrated with buffer B, and eluted with a 0−1 M NaCl gradient over 700 mL. The MerB-containing fractions were pooled. To prevent aggregation, the buffer of the pooled fractions was adjusted to a final concentration of 20 mM Tris (pH 8.0) and 100 mM NaCl. The pooled fractions were then concentrated to 10 mL and applied in 0.5 mL injections to a Superose-12 (Amersham Biosciences) molecular weight column equilibrated with buffer C [10 mM sodium phosphate (pH 7.5), 100 mM NaCl, 1 mM EDTA, and 1 mM DTT]. MerB-containing fractions were stored at 4 °C in buffer C.

MerA Purification. The Tn21 MerA gene was obtained in the form of plasmid pNS2 (*10*) from Dr. Richard Meagher

[1] Abbreviations: DTT, dithiothreitol; L-DTT, 2*R*,3*R*-dithiothreitol; DTE, dithioerythritol; EDTA, ethylenediaminetetraacetic acid; HSQC, heteronuclear single quantum coherence spectroscopy; IPTG, isopropyl β-thiogalactoside; merbromin, (2,7,-dibromo-9-(o-carboxyphenyl)-6-hydroxy-3-oxo-3H-xanthen-4-yl)hydroxymercury; mersalyl, 3-(hydroxymercuri)-2-methoxypropyl carbonyl phenoxyacetic acid; NMR, nuclear magnetic resonance; PHMBA, *p*-hydroxymercuri benzoic acid; PHMSA, *p*-hydroxymercuri benzenesulfonic acid.

at the University of Georgia. Plasmid pGB5 was created by ligating the Xba I/Hind III fragment of pNS2 into expression vector pET-21b (Novagen) cut with the same two restriction enzymes. *Escherichia coli* BL21-DE3 cells were transformed with pGB5 and grown at 37 °C in LB broth with 0.1 mg/mL ampicillin. Upon reaching an OD of 1.0, the cultures were induced with 0.4 mM IPTG and incubated for another 2−3 h before harvesting. Purification was based on the procedure of Rinderle et al. (*26*) with modifications. The cells from 6 L of culture were harvested by centrifugation in a Beckman JA-10 rotor at 5000*g* for 20 min, suspended in 200 mL of buffer A [20 mM Tris (pH 8.0), 1 mM EDTA, and 1 mM DTT] plus 1 mg/mL benzamidine, and then lysed by passage through a French press. The lysate was cleared by centrifugation at 100000*g* and applied to a DEAE-sepharose Fast Flow (Amersham Biosciences) column (50 mm i.d. × 40 cm length) equilibrated with buffer A, and MerA was eluted with a salt gradient of 0−1 M NaCl over 1.5 L. MerA-containing fractions were identified by the kinetic assay described below. Active fractions were pooled and dialyzed with a 10K cutoff membrane into buffer B [20 mM sodium phosphate (pH 7.2), 1 mM EDTA, and 1 mM DTT] and then applied to a Blue Sepharose Fast Flow (Amersham Biosciences) column (1.5 in. i.d. × 3 in. length) equilibrated with buffer B, and eluted with a 0−1 M NaCl gradient over 700 mL. Active fractions were concentrated to 10 mL and separated on a 200 mL Superdex-75 gel filtration column equilibrated with buffer D [10 mM sodium phosphate (pH 7.3), 1 mM EDTA, 1 mM DTT, and 100 mM NaCl]. MerA-containing fractions were reconcentrated to 5 mL, reduced with additional DTT, and then applied in 0.5 mL batches to a disposable PD-10 sephadex G25 desalting column (Amersham Biosciences) equilibrated with a storage buffer consisting of 50 mM sodium phosphate (pH 7.0), 100 mM NaCl, and 30% glycerol. The column eluent was immediately divided into 0.5 mL aliquots and stored at −80 °C.

NMR Spectroscopy. Purified MerB samples were concentrated to 0.5 mL at a final concentration of 1 mM by centrifugation in a 10K cutoff Centricon ultrafiltration device (Millipore). The samples were exchanged into an NMR buffer consisting of 10 mM sodium phosphate (pH 7.5), 10 mM NaCl, 1 mM EDTA, and 5−10 mM DTT by three cycles of dilution to 2.5 mL and reconcentration. D_2O was added to a final concentration of 10% to all samples before NMR experiments were performed. The MerB/Hg/DTT complex was prepared by adding at least one equivalent of an organomercurial substrate to an NMR sample of the free protein. Organomercurial substrates were all purchased from Sigma-Aldrich. The substrates used were as follows: phenylmercuric acetate [PMA; (62-38-4)], mersalyl (492-18-2), PHMBA (1126-48-3), merbromin (129-16-8), and PHMSA (17781-34-9). MerB/Hg/DTT samples with optically active L-DTT were prepared by diluting a MerB/Hg/DTT sample with L-DTT-containing buffer and reconcentrating it several times. The MerB/Hg/DTE samples were prepared in the same way. L-DTT and DTE were from Sigma-Aldrich. Gradient-enhanced two-dimensional (2D) $^{1}H-^{15}N$ HSQC spectra (*27*) were collected on a 600 MHz Varian Inova spectrometer. The NMR data were processed with NMRPipe/NMRDraw (*28*). The contour plots were prepared with gri (http://gri.sourceforge.net/).

X-ray Absorption Spectroscopy (XAS). A MerB/Hg/DTT sample was prepared by adding 1.5 equiv of PHMSA in the presence of 5 mM fresh DTT. This sample was concentrated to 2 mM and a final volume of 0.5 mL in a 10K cutoff Centricon device (Millipore). This sample was then exchanged into 10 mM sodium phosphate (pH 7.5), 20% v/v glycerol, by increasing the volume to 2.5 mL and reconcentrating it three times. This procedure also separated unbound mercury, PHMSA, and DTT from the protein. The sample was loaded into a 24 mm × 3 mm × 2 mm polycarbonate cuvette (with one 24 mm × 3 mm wall consisting of 0.001 in. Mylar tape) and immediately frozen in liquid nitrogen. X-ray absorption spectra were collected at the Stanford Synchrotron Radiation Laboratory (SSRL) on beamline 7-3 with the SPEAR ring operating at 3.0 GeV and 60−100 mA. The fluorescence excitation spectra were recorded with the sample at 10K using 1 mm vertically apertured beam incident on a Si[220] double-crystal monochromator that was detuned to 50% maximum reflectivity for harmonic rejection. The averaged XAS data represent eight scans, each of 21 min duration. EXAFSPAK software (www-ssrl.slac.stanford.edu/exafspak.html) was used for data reduction and analysis, according to standard procedures (*29*). The Fourier transforms (FTs) of the EXAFS spectra were generated using sulfur-based phase correction.

Kinetic Assays. MerA activity was followed by monitoring the consumption of NADPH:

$$N(t) = [\mathrm{NADPH}]_o - [\mathrm{NADPH}] \qquad (1)$$

where $N(t)$ is the total reaction progress. UV absorbance ($A_{340} = 6.22\ \mathrm{mM^{-1}\ cm^{-1}}$) was used to monitor the NADPH concentration. The reaction mixtures contained 50 mM sodium phosphate (pH 7.0), 100 mM NaCl, 100 μM NADPH, 1 mM cysteine, and varied concentrations (0−10 μM) of Hg(II) or MerB/Hg/DTT substrate. The assays were performed at room temperature. The reactions were initiated by adding 20 μL of a MerA aliquot to 1 mL of reaction mixture. The mixtures were well-mixed before recording began. Each MerA aliquot was thawed immediately before use. One aliquot was used for a series of 10 experiments plus 2−3 control experiments. The control experiments contained 4 μM Hg(II) as a substrate.

The MerB/Hg/DTT samples for use as MerA substrates in kinetic assays were prepared by adding 1.5 equiv of PHMSA to a sample of purified MerB in the presence of fresh DTT. To remove excess mercury, organomercurial, and DTT from the buffer, the complex was purified by injecting 5−8 mL on a sephadex G-25 gel filtration column with a void volume of 12 mL. A 10 mL fraction after the void volume was collected as the protein-containing fraction. Because residual DTT, mercury, or PHMSA in the MerB/Hg/DTT sample could potentially interfere with the assay results, we indirectly determined the degree of separation between protein and small molecules by using riboflavin as a tracer. Because riboflavin has a strong visible absorbance at ∼450 nm, its concentration in the MerB-containing fraction was easily measured. By this measure, the degree of separation between riboflavin and protein was at least 1:1000. Other small molecules such as unbound mercury, organomercurials, and DTT should behave in a similar way.

A stock of free MerB free of contaminating NADPH oxidase activity was prepared for use in enzyme buffering

tests. A 10 mL sample of purified MerB was dialyzed into 20 mM sodium phosphate (pH 7.4), 1 mM EDTA, and 1 mM DTT and then applied to a Blue Sepharose Fast Flow (Amersham Biosciences) column (1.5 in. i.d. × 3 in. length) equilibrated with the same buffer. MerB was collected from the flow-through of this column. No significant NADPH oxidase activity was detected in this MerB stock. Aliquots were freshly reduced and separated from DTT before use in kinetic assays by the following procedure. DTT was added to a final concentration of 4 mM to an 0.5 mL aliquot of 0.5 mM free MerB. The aliquot was then injected onto a PD-10 desalting column, and 1.5 mL of MerB-containing eluent was collected for use in enzyme buffering tests. The free MerB stock was used within 4 h of preparation and kept on ice until use in the assays.

Analysis of Kinetic Data. As noted in several other multiple turnover studies of MerA activity, the reaction proceeds with a rapid initial velocity, which decays to a slower, constant final velocity (see Discussion). The change in velocity cannot be ascribed simply to substrate depletion or product buildup, because it can happen before substrate concentrations change significantly. The change can be explained by conversion of enzyme between a more active and a less active form, the rate of conversion being dependent on thiol and substrate conditions. The reaction velocity will then follow an exponential course (*26*):

$$v = v_f + (v_o - v_f)e^{-kt} \quad (2)$$

where v_f is the final steady state velocity, v_o is the initial rapid velocity, and k is the net rate of conversion between the two MerA forms. The total reaction progress (which is the quantity measured in MerA assays) is obtained by integrating eq 2 to obtain:

$$N(t) = \int_0^t v(t) = v_f t - \frac{v_o - v_f}{k}e^{-kt} + \frac{v_o - v_f}{k} \quad (3)$$

All measured reaction curves were fitted to eq 3 by adjusting the parameters v_f, v_o, and k. The normalized, relative activity v_o^{rel} is defined as the ratio of v_o for that assay to the average v_o for the control experiments [4 μM Hg(II)] in that assay series. This ensures that any differences in MerA activity between aliquots do not affect the comparison of measurements taken using different aliquots.

RESULTS

Preparation of a Stable MerB/Hg/DTT Complex. To elucidate the structure and mechanism of MerB, we wanted to prepare a stable complex of MerB involving either an organomercurial substrate or a mercuric ion. At pH 7.5 and in the presence of fresh DTT, free MerB adopts a single, well-folded conformation, as shown by the 2D $^1H-^{15}N$ HSQC spectrum (Figure 2A). The spectral quality deteriorated quickly in the absence of DTT, even in the presence of other reducing agents such as cysteine or glutathione. Because DTT was essential for the formation of a well-folded stable NMR sample and because DTT is a known inhibitor of MerB's catalytic activity, we used the above conditions as a starting point for the formation of a stable mercury-containing MerB complex.

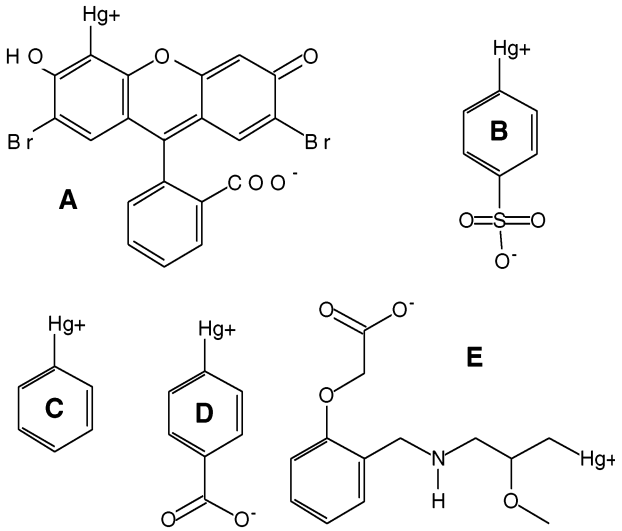

FIGURE 1: Organomercurial substrates used to prepare the MerB/Hg/DTT complex: (A) merbromin, (B) PHMSA, (C) PMA, (D) PHMBA, and (E) mersalyl.

A mercury-containing MerB complex was prepared by adding the organomercurial substrate PHMBA to a sample of free MerB in the presence of DTT. The resulting 2D $^1H-^{15}N$ HSQC spectrum (Figure 2B) is very similar to the spectrum of the free form (Figure 2A); we observed significant chemical shift changes for only a few signals. These results indicate that the global fold of the protein remains the same upon interaction with the organomercurial substrate.

This procedure was repeated with a variety of organomercurial substrates (Figure 1). We expected that the resulting $^1H-^{15}N$ HSQC spectra would display significant differences depending on which substrate was used, because binding of these substrates with various aromatic ring structures should have affected the chemical shifts of the MerB binding surface in different ways. Surprisingly, the resulting $^1H-^{15}N$ HSQC spectra were identical for all substrates tested (Figure 2B), indicating that the organic portion of these organomercurial substrates was not present in the MerB complex. To confirm this result, we prepared a MerB complex using only free Hg(II) as a substrate; the resulting spectrum was identical to those obtained using samples prepared with organomercurial substrates (Figure 2B). When complexes were prepared with substrate-to-protein ratios ranging from 1 to 2.5, the resulting spectra were also identical. Extensive buffer exchange or dilution and reconcentration of the MerB complex in the absence of additional mercury or organomercurial did not change the spectrum either. Therefore, a mercuric ion binds to MerB to form a very stable complex with a 1:1 stoichiometry. Overall, these results suggest a mechanism by which organomercurials are cleaved rapidly by MerB to form a stable mercury-containing MerB complex in the presence of DTT.

Multiple NMR data demonstrate that DTT is also present in the MerB complex. We prepared a 1 mM MerB complex with $^{13}C/^{15}N$-labeled MerB, unlabeled DTT, and PHMSA, and this complex was extensively dialyzed to remove excess DTT and PHMSA. The sample contained 1 mM EDTA. A one-dimensional ^{13}C-filtered spectrum of this complex clearly shows a resonance at the chemical shift of the magnetically equivalent H2 and H3 protons of free DTT (not shown). The

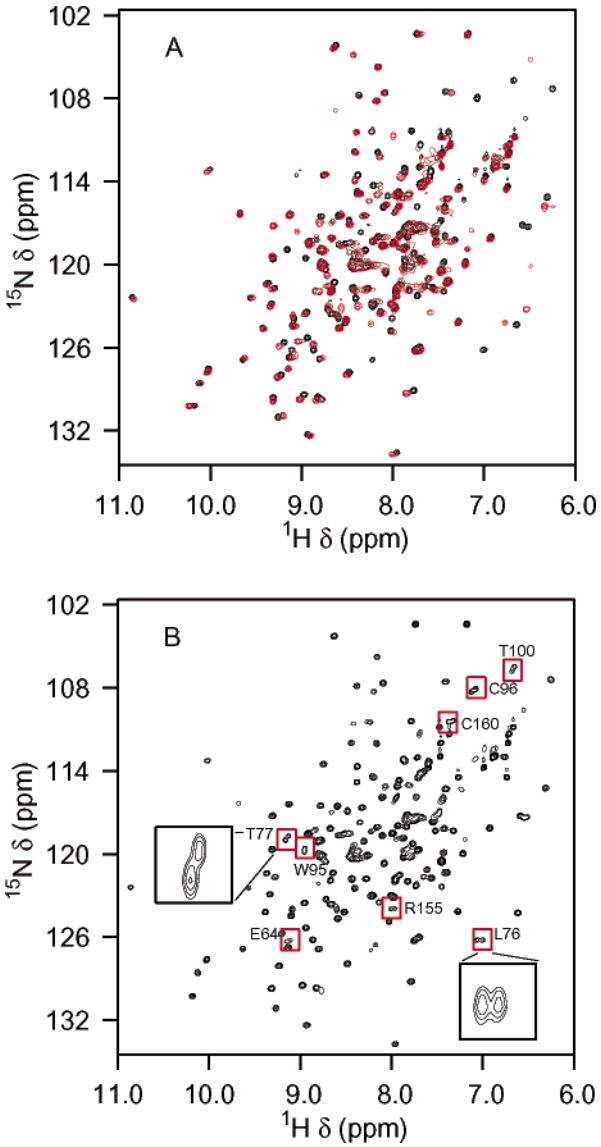

FIGURE 2: (A) Two-dimensional ^{1}H−^{15}N HSQC spectra of free MerB (red) and of the MerB/Hg/DTT complex prepared with L-DTT (black). (B) Two-dimensional ^{1}H−^{15}N HSQC spectrum of the MerB/Hg/DTT complex prepared with racemic DTT. The boxes indicate signals that appear as paired peaks in the presence of racemic DTT but as single peaks in the presence of L-DTT.

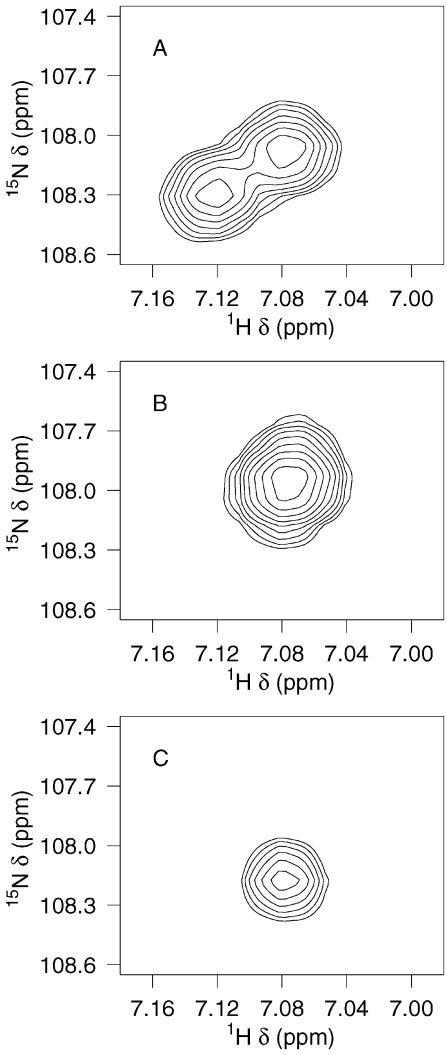

FIGURE 3: Evidence for the MerB/Hg/DTT complex. Region of the 2D ^{1}H−^{15}N HSQC spectrum of the ^{15}N-labeled MerB/Hg/DTT complex at 27 °C when it is prepared with (A) racemic DTT, (B) L-DTT, or (C) DTE. The peak(s) shown correspond to the amide signals of residue C96.

ratio of the integration of the H2/H3 peak (two protons) from DTT to the integration of the EDTA peak at 3.2 ppm (four protons) was 0.53, which is very near the ratio of 0.5 expected for a 1:1 mixture of DTT and EDTA. The MerB complex therefore contains 1 equiv of mercury as well as 1 equiv of DTT and is therefore termed the MerB/Hg/DTT complex. There is also indirect evidence from 2D ^{1}H−^{15}N HSQC spectra that DTT is present. One feature of the MerB/Hg/DTT spectrum not seen in the free protein spectrum is the presence of several closely spaced pairs of peaks (Figure 2B). The two peaks of each pair are of approximately equal intensity. When the complex is prepared with pure optically active L-DTT instead of a 50/50 racemic mixture of DTT, only one member of each pair of peaks remains (Figure 3A,B). The paired peaks belong to residues affected by the binding of DTT and arise from the fact that MerB/Hg/L-DTT and MerB/Hg/D-DTT have slightly different spectra. Sequence specific assignments of most backbone amide resonances have been obtained as part of the solution structure determination of the MerB/Hg/DTT complex by NMR (*30*). Eight of the paired peaks have been assigned to the residues E64, L76, T77, W95, C96, T100, R155, and C160. No such pairing of peaks occurs in the free protein spectrum in the presence of DTT (Figure 2A), which indicates that DTT does not associate with the free protein. Furthermore, this implies that the association of the DTT molecule to the protein is mediated by the mercury atom. The DTT molecule could associate with the mercury atom either through only one of its sulfurs in a linear conformation or through both of its sulfurs in a cyclic conformation. To distinguish between the cyclic and the linear binding modes, we have prepared analogous complexes with the *meso* compound DTE, which is not chiral, but otherwise chemically equivalent to DTT. There are two possible linear MerB/Hg/DTE complexes but only one possible cyclic MerB/Hg/DTE complex (Figure 4). Because the two linear forms are diastereomers, they would have different NMR spectra, and the MerB/Hg/DTE spectrum would exhibit paired peaks similar to those seen in the presence of a racemic mixture of DTT. The pairing of peaks does not occur in the MerB/Hg/DTE spectrum (Figure 3C). The observation of only a

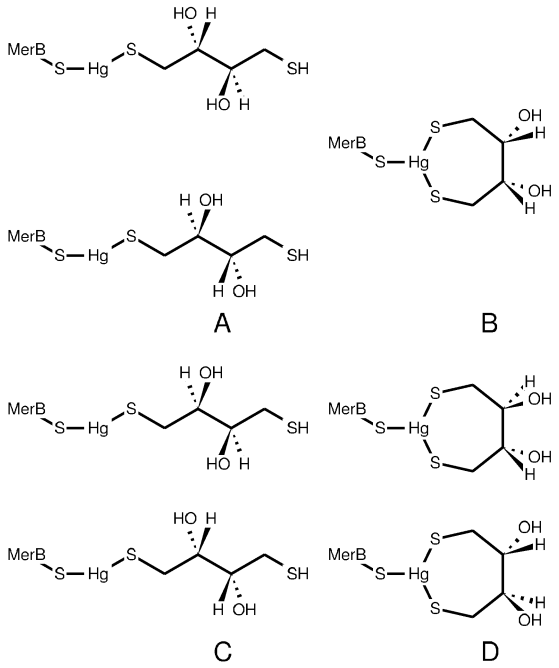

FIGURE 4: (A) Two possible linear binding modes of DTE in the MerB/Hg/DTE complex. The two possible complexes are diastereomers and lead to two distinct populations in the NMR spectrum. (B) In the cyclic binding mode, only one MerB/Hg/DTE complex is possible, leading to a single population in the NMR spectrum. (C) There are two possible linear MerB/Hg/DTT complexes, leading to two populations in the spectrum. There are also two distinct cyclic MerB/Hg/DTT complexes (D), leading to two populations in the spectrum.

Table 1: Curve Fitting Results for Hg EXAFS of the MerB/Hg/DTT Complex[a]

sample filename (k range) $k^3\chi$	fit	shell	R_{as} (Å)	σ_{as}^2 (Å)	ΔE_0 (eV)	f' [b]
MerB/Hg/DTT	1	Hg−S	2.42	−0.0010	−3.93	0.103
HBDTA (2−12 Å^{-1})	2	Hg−S_2	2.42	0.0025	−1.91	0.091
$k^3\chi = 10.74$	3	Hg−S_3	2.43	0.0051	−0.73	0.092
	4	Hg−S_4	2.43	0.0074	−0.02	0.099

[a] Shell is the chemical unit defined for the multiple scattering calculation. Subscripts denote the number of scatterers per metal. R_{as} is the metal−scatterer distance. σ_{as}^2 is a mean square deviation in R_{as}. ΔE_0 is the shift in E_0 for the theoretical scattering functions. [b] f' is a normalized error (χ^2): $f' = (\{\sum_i[k^3(\chi_i^{obs} - \chi_i^{calcd})]^2/N\}^{1/2})/[(k^3\chi^{obs})_{max} - (k^3\chi^{obs})_{min}]$.

single peak with DTE is only consistent with a cyclic conformation, bound to the mercury through both sulfur atoms (Figure 4B).

EXAFS Studies of the MerB/Hg/DTT Complex. To determine the geometry of ligands associated with the Hg(II), EXAFS data were collected on the MerB/Hg/DTT complex. The EXAFS data of the MerB/Hg/DTT complex are most consistent with a coordination sphere for mercury consisting of three sulfur atoms (Table 1 and Figure 5). The measured Hg−S bond distance of 2.42 Å coincides with other mononuclear, mercuric−thiolate compounds that have a coordination number of three (*31*). A search of the Cambridge Structural Database has confirmed that the Hg−S bond length is a sensitive indicator of coordination number: di-, tri-, and tetra-coordinate mononuclear mercuric−thiolate complexes have Hg−S bond lengths of 2.34 ± 0.02, 2.44 ± 0.04, and 2.54 ± 0.03 Å, respectively (Table 2). Also, although models

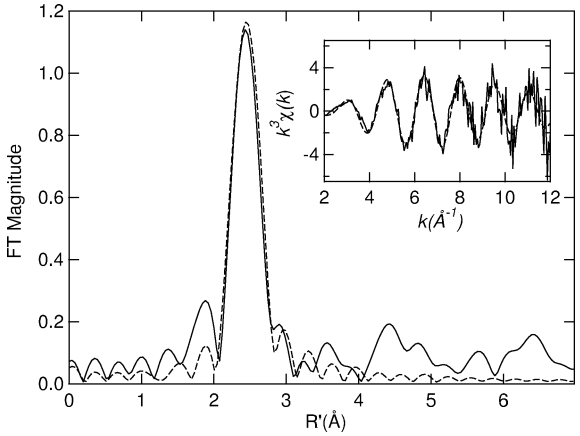

FIGURE 5: FTs of the Hg L_3 EXAFS of MerB/Hg/DTT (solid) and theoretical best fit (dashed) corresponding to a coordination shell of HgS_3 using the parameters of fit 3, Table 1. The k^3-weighted EXAFS (solid) and theoretical best fit (dashed) are displayed as insets.

Table 2: Hg−S Bond Distances of Representative 2-, 3-, and 4-Coordinate HgS Compounds[a]

CSD code	Hg−S_2	CSD code	Hg−S_3	CSD code	Hg−S_4
BEPQAO	2.30	DELFIG	2.43	BULZUD	2.55
	2.30		2.40		2.53
BINMIU	2.36		2.51		2.52
	2.36	JEFVIZ	2.45		2.55
JETYOW	2.35		2.44	LAJGUY	2.52
	2.35		2.44		2.52
JAPROH	2.36	KELVUS	2.40		2.52
	2.36		2.46		2.52
KELWEP	2.32		2.47	NIRJIH	2.51
	2.32	KINZAI	2.40		2.54
MECBHG	2.35		2.49		2.60
	2.35		2.40		2.53
NUCFIA	2.34	VOXTOR	2.46	TPTCHG	2.51
	2.34		2.40		2.55
MEPMEP10	2.33		2.48		2.58
	2.33				2.49
MERSET01	2.34			WEMTOX	2.54
	2.34				2.56
MERMES	2.36				2.55
	2.36				2.57
NEHDOT	2.33			SLINIK	2.56
	2.35				2.56
					2.55
					2.56
average[b]	2.34 ± 0.02		2.44 ± 0.04		2.54 ± 0.03

[a] Representative mononuclear mercuric thiolate compounds were taken from the Cambridge Structural Database (CSD). Bond lengths are reported in angstroms. [b] Mean bond length ± standard deviation.

with two, three, or four sulfurs all can provide good fits to the data, the Debye−Waller value (σ_{as}^2) for the HgS_3 case is the most physically reasonable one. Taken together, the NMR and EXAFS data are consistent with a model for the MerB/Hg/DTT complex in which two sulfurs from DTT and one sulfur from the protein bind to the mercuric ion.

Cysteine C_β Chemical Shift. The chemical shifts of the C_β atoms of all four cysteine residues in the MerB/Hg/DTT complex have been determined as part of the three-dimensional structure determination (*30*). The C_β chemical shifts of the cysteine residues provide evidence that C96 is the only cysteine involved in mercury binding in the MerB/Hg/DTT complex. This cysteine residue has been shown to be critical for MerB catalysis (*17*). In the free protein, C117,

Table 3: C_β Chemical Shift (ppm) for Cysteine Residues in the MerB/Hg/DTT Complex and in Free MerB

residue	MerB/Hg/DTT complex	free MerB
C96	37.9	*a*
C117	29.7	29.8
C159	32.8	28.3
C160	26.7	27.0

[a] Not observed.

C159, and C160 all display standard C_β chemical shifts for reduced cysteines, and the chemical shift of C96 C_β was not assigned. In the MerB/Hg/DTT complex, the C_β shifts of C117, C159, and C160 are also in the standard range for reduced cysteine, but for C96, the C_β shift (37.9 ppm) is unusually downfield (Table 3). The downfield C_β shift of C96 could be explained by formation of a disulfide bond involving this residue (*32*), but it is unlikely that such a disulfide bond is present given the absence of available thiol groups. Indeed, no free thiol is available in the buffer, there is no evidence that other cysteines in the MerB monomer form a disulfide bond, and there is no evidence from our studies that the MerB/Hg/DTT complex forms a dimer. The more likely explanation for the chemical shift of C96 C_β is coordination to the mercuric ion. Cysteine C_β chemical shifts are sensitive to mercuric ion binding at the thiolate group. In solution NMR studies of $Hg(SR)_n$ complexes, C_β generally shifts downfield as the number of thiol ligands (n) increases (*33*). The observed chemical shift of C96 C_β in the MerB/Hg/DTT complex is consistent with a population of essentially 100% HgS_3 (see Table 3). The C_β chemical shift of C159 is slightly downfield from the standard range for reduced cysteine (Table 3) but much less so than that of C96. This observation allows the possibility of a small degree of exchange between C96 and C159. In the solution structure of the MerB/Hg/DTT complex (Benison, G. C., Di Lello, P., Legault, P., and Omichinski, J. G. Unpublished results), the distance between the sulfur atoms of C159 and C96 is 9 Å, which is close enough to allow for some exchange.

Other MerB/Hg/Thiol Complexes. Because DTT is a known inhibitor of MerB but it is not a naturally occurring molecule, we performed several experiments designed to produce a mercury-containing MerB complex involving a physiological thiol such as cysteine or glutathione. When an organomercurial substrate is added to a MerB sample in the presence of one of these monothiols and in the presence of oxygen, the result is a $^1H-^{15}N$ HSQC spectrum with very poor chemical shift dispersion (not shown). This is probably because these thiols are not able to keep the protein in a fully reduced state at the high concentrations needed for NMR studies. We also performed experiments in which organomercurial substrates were added to a mixture of reduced MerB and cysteine or glutathione in an anaerobic environment. This resulted in spectra with improved chemical shift dispersion nearly equivalent to that seen in the MerB/Hg/DTT complex, but the spectra were not as reproducible as that of the MerB/Hg/DTT complex. The exact composition of these complexes also is not clear, as it is for the MerB/Hg/DTT complex. Because of its excellent stability, homogeneity, and reproducibility, we used the MerB/Hg/DTT complex for further kinetic and structural studies.

Table 4: Determination of K_D for the MerB/Hg/DTT Complex by NMR[a]

thiol	f (%)	K_D
none	<15	<26 nM
1 mM cysteine	<15	<26 nM
10 mM cysteine	65	1.6 μM

[a] The stability of the MerB/Hg/DTT complex was determined by monitoring the equilibrium between the free MerB and the MerB/Hg/DTT complex by NMR, under various thiol conditions. f is defined as in eq 4.

Enzyme Buffering Tests. We performed a series of experiments designed to test the hypothesis that the mercuric ion product of MerB can pass directly to MerA without diffusing through the cytosol. A variety of methods have been developed to identify this type of transfer. The method that we use here has been termed the enzyme buffering test (*34*). There are three components to this test, which in our case are as follows: a measurement of the K_D of MerB for the mercuric ion, a measurement of the kinetic parameters (K_M and v_{max}) of MerA with a mercuric ion substrate, and a measurement of MerA activity with the MerB/Hg/DTT complex as a substrate. We performed these experiments in the presence of 1 mM cysteine because this reflects the physiological situation and because all reported multiple turnover studies of MerA to date require the presence of cysteine or another single sulfhydryl small molecule.

Measurement of K_D. The dissociation constant of the MerB/Hg/DTT complex was measured under several thiol conditions (Table 4). An aliquot of 1 mL of ~1 mM MerB/Hg/DTT was dialyzed into 1 L of buffer, and the appearance of free MerB was monitored by NMR spectroscopy. Prior to dialysis, all unbound DTT was removed from the MerB/Hg/DTT sample by several rinses and reconcentrations with DTT-free buffer. A 2D $^1H-^{15}N$ HSQC spectrum was collected at this point to ensure that the MerB/Hg/DTT complex was intact before dialysis. Dialysis was performed in a disposable, 2 mL, 10K cutoff tube (Spectrum Laboratories). The concentrations of free protein, bound protein, and free mercury are controlled by the dissociation constant K_D:

$$K_D = \frac{[\text{MerB}] \times [\text{Hg/DTT}]}{[\text{MerB/Hg/DTT}]} = \frac{f^2}{(1-f)} \frac{v_i}{v_o} [\text{MerB/Hg/DTT}]_o \quad (4)$$

where f is the fraction of MerB/Hg/DTT that has dissociated, v_i is the volume containing protein, v_o is the volume of the dialysis buffer, and $[\text{merB/Hg/DTT}]_o$ is the initial concentration of MerB/Hg/DTT being dialyzed. The fraction f can be measured by NMR because free MerB and MerB/Hg/DTT have distinct 2D $^1H-^{15}N$ HSQC spectra. The dialysis was allowed to proceed for 24 h before NMR measurements were made. When none of the free form was observed in a spectrum, the parameter f was set to a lower bound of 15%. This number is based on the minimum reversion to the free form that would be clearly visible in the spectrum given its signal-to-noise ratio. Because the total amount of MerB present in the system remains constant, the quantity $[\text{MerB/Hg/DTT}]_0 \cdot v_i$ in eq 4 is constant; i.e., a change

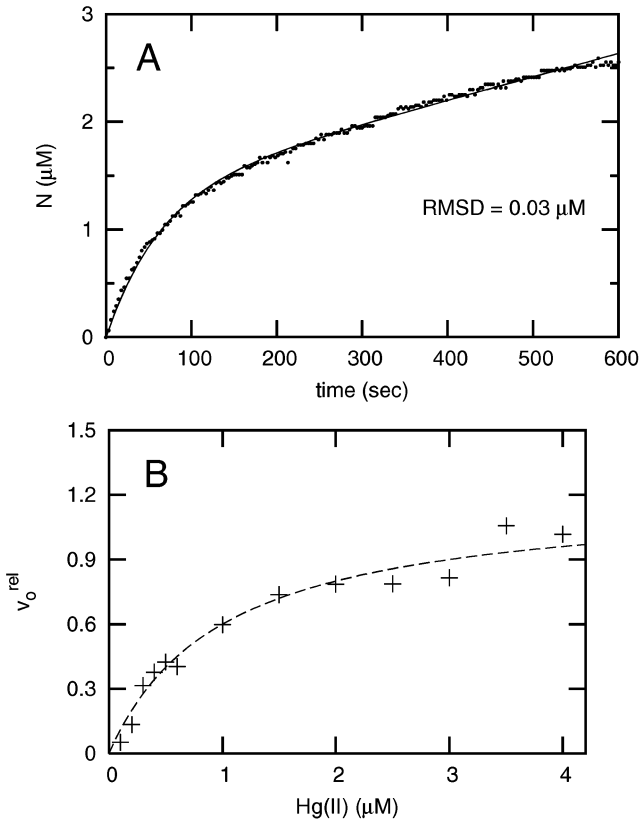

FIGURE 6: (A) Typical reaction curve for the MerA assay. The reaction contained 1 mM cysteine and 9.3 μM MerB/Hg/DTT complex as a substrate, plus standard components described in the Materials and Methods. The fitted line corresponds to eq 3 with the parameters $v_o = 23.3$ nM s^{-1}, $v_f = 2.1$ nM s^{-1}, $k = 0.015$ s^{-1}. The RMSD between the observed $N(t)$ and the calculated $N(t)$ for this particular curve is 0.03 μM. (B) Measurement of MerA kinetic properties with Hg(II) substrate. The initial velocity was determined using eq 3 and normalized to a control experiment as described in the Materials and Methods. Assays contained 1 mM cysteine. The fitted line corresponds to $K_M = 1.0$ μM, $v_{max}^{rel} = 1.2$. v_{max}^{rel} is a unitless ratio as described in the Materials and Methods.

in v_i due to a change of buffer volume during dialysis is exactly counteracted by an opposite change in dialysate concentration.

Table 4 shows the results of the K_D measurements under several thiol conditions. The condition with 1 mM cysteine is the most important for this study, because that is the condition used in the enzyme buffering tests to follow. No dissociation was detected in the presence of 0−1 mM cysteine, leading to an upper bound of 26 nM for the apparent K_D (Table 4). The measurement of an apparent K_D of 1.6 μM in the presence of 10 mM cysteine indicates that the dialysis method is capable of showing dissociation and that at a sufficiently high concentration, cysteine is capable of removing mercury from the MerB/Hg/DTT complex.

MerA Assays with Hg(II) Substrate. All kinetic traces were fit to eq 3 as described in the Materials and Methods. The quality of fit was determined from the sum of squared residuals between the data and the predicted values from eq 3. For all experiments used in the kinetic analysis, the RMSD between the observed and the expected values was below 0.05 μM (i.e. $\chi_n^2 < 1$ for a 0.05 μM error in NADPH concentration measurement.) A typical fit with an RMSD value of 0.03 μM is shown in Figure 6A.

Table 5: MerA Velocity Using MerB/Hg/DTT as a Substrate[a]

[MerB/Hg/DTT] (μM)	v_o (nM s^{-1})	n
10	6.9 ± 1.2	3
15	7.8 ± 1.2	4
20	6.3 ± 2.2	3

[a] Assays contained 14 nM MerA. v_o is the initial velocity, reported as mean and standard deviation. n is the number of replicates.

The kinetic parameters of MerA with a mercuric chloride substrate were measured in a series of assays. All assays contained 1 mM cysteine, and a series of mercuric chloride substrate concentrations from 0 to 4 μM were used. The results are shown in Figure 6B. The activity was fit to a Michaelis−Menten model with parameters $K_M = 1.0$ μM, $v_{max}^{rel} = 1.2$. v_{max}^{rel} is in the unitless scale described in the Materials and Methods (i.e., the activity at 4 μM Hg(II) is 1.0 by definition).

Although it is the relative velocity, and not the absolute velocity, that is needed for the enzyme buffering tests, we also measured the absolute velocity for the purpose of comparison with other studies. A MerA concentration of 0.7 μM was measured in one aliquot by absorbance at 455 nm, using a value of $\epsilon_{455} = 11.3$ mM^{-1} cm^{-1} (*26*). Because the aliquots were diluted by a factor of 50 in the assays, the final concentration of MerA in the assays was 14 nM. The average value of v_o in the control experiments with 4 μM Hg(II) was 24 nM s^{-1}. The value of v_{max}^{rel} was 1.2 (see Figure 6B), so the absolute value of v_{max} is 28.8 nM s^{-1}. The specific activity, obtained by dividing the absolute v_{max} by the MerA concentration, was 123 min^{-1} for our MerA preparation.

MerA Assays with MerB/Hg/DTT Substrate. Two series of MerA assays were performed using the MerB/Hg/DTT complex as a substrate. As described in the Materials and Methods, the only source of mercury in these assays was that bound to MerB. Excess free mercury was removed from the MerB/Hg/DTT complex by gel filtration prior to the assays, and no free mercuric substrate was added to the assays. The MerB/Hg/DTT concentration (10−30 μM) was several orders of magnitude larger than the MerA concentration (14 nM). In the first series of assays, several MerB/Hg/DTT concentrations were tested in several replicates (Table 5). On the basis of these results, the velocity measurements under these conditions are accurate to within approximately 20%. In the second series of assays, the reaction mixtures contained an initial concentration of 9.3 μM MerB/Hg/DTT and varied amounts of free excess MerB. These assays were done in parallel with control assays using 4 μM Hg(II) as a substrate, to allow the calculation of a normalized v_o^{rel}. For each assay, an expected free mercury concentration $[Hg(II)]_{calcd}$ was calculated on the basis of eq 4 and the K_D value in Table 4. Note that "free" Hg(II) in this sense means Hg(II) not bound to protein, although it is bound to whatever small thiol is present. We then calculated an expected MerA velocity based on $[Hg(II)]_{calcd}$. For all concentrations of free MerB used, the observed velocity was higher than what is expected from a purely dissociative mechanism, sometimes by a factor of as high as 9 (Table 6).

Table 6: Enzyme Buffering Tests of MerA Velocity in the Presence of MerB/Hg/DTT and Free MerB[a]

free MerB (μM)	$Hg(II)_{calcd}$ (μM)	v^{rel}_{calcd}	v^{rel}_{obs}	$v^{rel}_{obs}/v^{rel}_{calcd}$
0	0.47	0.38	0.69	1.82
0.9	0.21	0.20	0.43	2.15
1.8	0.12	0.13	0.37	2.87
2.7	0.08	0.09	0.46	5.11
3.6	0.06	0.07	0.62	8.86
4.5	0.05	0.05	0.27	5.40
5.4	0.04	0.05	0.45	9.00
9.1	0.02	0.03	0.28	9.33

[a] All assays contained 14 nM MerA, 9.3 μM MerB/Hg/DTT, and varied amounts of free excess MerB (0−9.1 μM). $Hg(II)_{calcd}$ was determined from the K_D reported for 1 mM cysteine in Table 4. v^{rel}_{calcd} was determined as described in the text. v^{rel}_{obs} is the measured MerA velocity (reported as a unitless ratio as described in the Materials and Methods).

DISCUSSION

DTT Inhibits MerB. It has been observed previously that DTT inhibits MerB (*16*, *17*), but the mechanism of the inhibition was not clearly understood. Using NMR experiments, we have demonstrated that the inhibition is due to the formation of a stable MerB/Hg/DTT complex. Our results demonstrate that DTT does not inhibit the cleavage of the carbon−mercury bond but rather prevents the release of the mercuric ion product. On the basis of EXAFS and NMR spectroscopy experiments, we conclude that the mercury in the MerB/Hg/DTT complex is bound in a coordination sphere consisting of three sulfur atoms and that two of the sulfur atoms originate from DTT. The third sulfur atom is from C96 of MerB. The MerB/Hg/DTT complex is extremely stable. Our attempts to competitively remove the bound DTT with the naturally occurring monosulfhydryl-containing compound cysteine required extremely high ratios of cysteine to DTT (Table 4).

The two isomers of DTT form the MerB/Hg/DTT complex with approximately equal affinity as judged by the HSQC spectrum. In other words, MerB exhibits little if any chiral specificity for its DTT cofactor. This is consistent with the idea that the primary interaction between the DTT molecule and the protein is through the mercuric ion and the sulfur atoms and that the interaction of the remainder of the DTT molecule and the protein is of minor importance for binding. The ability of MerB to accept both enantiomers suggests that the binding site for DTT is larger than DTT or is not very well-ordered, which is consistent with the wide thiol cofactor acceptance of MerB.

Kinetics of MerA Reaction. MerA is very similar in structure and mechanism to the other members of the disulfide oxidoreductase family, but what distinguishes MerA is its ability to reduce mercuric ions at a catalytically useful rate. Mercuric ions rapidly inactivate other members of this enzyme family by binding to the sulfhydryl groups. It has been shown that mercuric ions can also inactivate MerA in this fashion to a smaller degree, with the degree of inactivation depending on the conditions. An inactivated form of MerA was isolated in a single turnover experiment in which mercuric cyanide was the substrate, and there were no thiols present (*22*). The inactivated form was shown to involve mercuric ions simultaneously bound to both the inner, active site cysteine pair and the carboxyl-terminal cysteine pair.

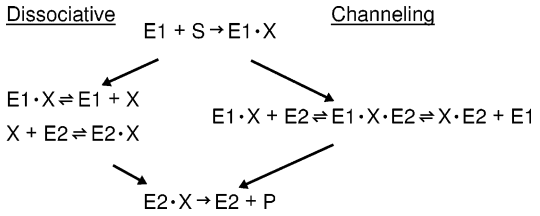

FIGURE 7: Dissociative vs channeling mechanism for metabolite transfer in sequential reactions, using the notation of Ovadi (*50*). The initial substrate S is converted into the final product P by two sequential enzymatic reactions catalyzed by enzymes E1 and E2. The intermediate metabolite X is the product of the reaction catalyzed by the enzyme E1. X is also the substrate for the reaction catalyzed by the enzyme E2. In the dissociative mechanism (left), the E1−X complex dissociates, yielding free X in solution. X then diffuses to and binds E2 in the second step. In the channeling mechanism (right), the E1−X complex binds E2 to yield a transient E1−X−E2 complex. E1 then dissociates from this complex to yield the X−E2 complex. In no part of the channeling mechanism does metabolite X exist freely in solution. In the present study, S = HgR, E1 = MerB, X = Hg(II), E2 = MerA, and P = Hg(0).

Under these conditions, approximately 50% of the enzyme accumulates in the inactivated state, and the other 50% completes a full catalytic cycle. It is probably because of this type of inactivation that no multiple turnover activity is observable in the absence of thiols. In the presence of thiols, multiple turnover activity is seen; however, it has been observed that the rate undergoes a steady decline, continuing over many turnovers, which cannot be explained by the simple depletion of substrates (*26*). One likely explanation for this behavior is that during each catalytic cycle, a small portion of the enzyme accumulates in an inactivated state similar to that seen in the mercuric cyanide experiment. In the present study, this change in rate was also observed. For example, in the typical trace seen in Figure 6A, by the time 50 turnovers are complete (corresponding to a substrate consumption of 0.7 μM), the rate has dropped to approximately half of its initial value. This would be the result expected if, upon each catalytic cycle, 1% of the enzyme were lost to accumulation in an inactivated form.

The derivation of eq 3 does not take into account the fact that substrate and product concentrations are changing during the course of the reaction. However, analysis of kinetic data and the enzyme buffering test was based entirely on consideration of initial reaction rates. So, the conclusions depend mainly on the ability of eq 3 to accurately describe the initial part of the reaction. For the initial part of the curve, the assumption that substrate concentrations are not very different from their initial values is valid. For example, in Figure 6A, it is apparent that the initial reaction rate is well-established when less than 10% of the substrate has been consumed. Equation 3 may indeed be a poor model for the reaction at longer times (>2 min) at low substrate concentrations. However, the RMSD measure and examination of the curves showed that eq 3 provided a good fit to the initial reaction velocity at all concentrations.

Reaction Scheme for MerA and MerB. Given the evidence presented here and evidence from previous studies, we present the model shown in Figure 8 for the detoxification of organomercurials by MerB and MerA. In a previous model, on the basis of a variety of biochemical experiments (*17*), the organomercurial substrate makes initial contact with C159 of MerB. C96 of MerB is then involved in cleavage

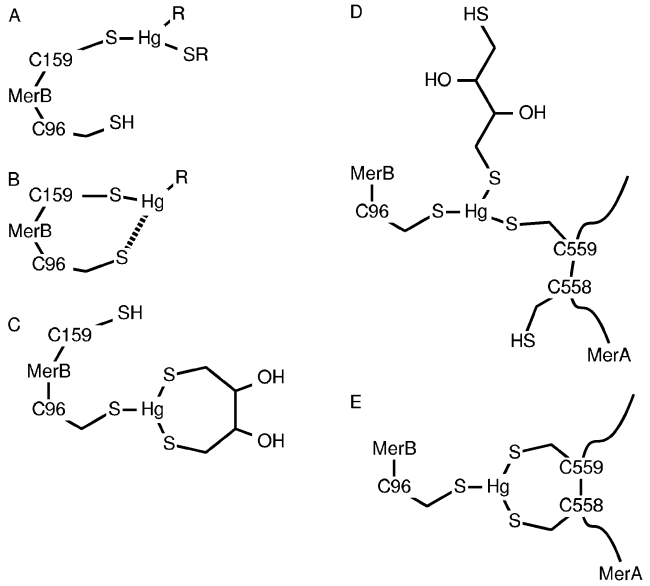

FIGURE 8: Proposed reaction mechanism including direct transfer of the mercuric ion to MerA. (A) C159 of MerB displaces the buffer thiol bound to the organomercurial substrate. (B) C96 catalyzes cleavage of the carbon−mercury bond. (C) The MerB/Hg/DTT complex forms with a molecule of DTT from the buffer. (D) The carboxyl-terminal cysteines of MerA displace the bound DTT molecule from the MerB/Hg/DTT complex. (E) The mercuric ion is transferred to MerA through a trigonal intermediate similar to the MerB/Hg/DTT complex.

of the carbon−mercury bond. In the present study, the mercuric ion then remains bound to C96 in the MerB/Hg/DTT complex (Figure 8C). Because the initial organomercurial substrate is certain to exist as an HgR/DTT complex, the question arises whether the DTT molecule present in the MerB/Hg/DTT complex is the same one present in the initial organomercurial/DTT substrate or whether it is a new one derived from the buffer. The present data are not sufficient to distinguish these possibilities. However, it has been shown that MerB can support a single turnover even in the absence of buffer thiols (*17*). This at least suggests that it is not necessary for the DTT molecule to remain bound to the organomercurial substrate throughout the reaction course and that the DTT molecule present in the MerB/Hg/DTT complex may be a new one derived from the buffer rather than the one initially bound to the HgR^+ substrate.

We propose that the direct transfer of the mercuric ion from MerB to MerA is achieved through a trigonal intermediate involving the carboxyl-terminal cysteines of MerA (Figure 8D,E). The highly conserved carboxyl-terminal cysteine pair of MerA has been shown to be required for the removal of tightly bound thiol ligands from mercuric ion substrates (*22*). Because MerB can be thought of as a very large, tightly bound thiol ligand, it is a reasonable hypothesis that the carboxyl-terminal cysteines of MerA are involved in removing the mercuric ion directly from MerB. Furthermore, the MerB/Hg/DTT complex demonstrates that MerB can accommodate a trigonal intermediate involving C96 of MerB and two exogenous sulfur atoms from another molecule (Figure 8C). An analogous intermediate may exist during MerB−MerA transfer, where the two carboxyl-terminal cysteines of MerA are the two exogenous sulfur atoms (Figure 8E).

Substrate Channeling. Such direct transfer of mercuric ions may occur in at least two other steps of the mercury detoxification process. MerP is a periplasmic protein that sequesters mercuric ions, and MerT is a transmembrane protein that transports mercuric ions across the cell membrane. There is evidence that mercuric ions are transferred directly from MerP to MerT through a trigonal intermediate, similar to the one observed in the MerB/Hg/DTT complex (*35*). It has also been proposed that the mercuric ion is transferred directly from the cytosolic side of MerT to MerA (*35*).

Direct transfer of mercuric ions between MerB and MerA, and between other proteins in the mercury resistance system, has important biological implications, as it would minimize the toxic effects of the intermediate mercuric ion on other cellular components. In fact, in the case of MerT and MerB, free release of mercuric ions seems counterproductive to the function of the proteins. For both proteins, the only known destination of the product is MerA. Furthermore, the product of MerB (a mercuric ion) is actually more reactive than the substrate (an organomercurial.) Direct transfer to MerA would prevent the need for free release of the toxic product of MerB.

The type of mechanism in which a metabolite passes directly between enzymes is known as substrate channeling (*36*). In the substrate channeling mechanism, the first enzyme E1 (using the notation in Figure 7) converts the initial substrate S into the intermediate X. X is then transferred directly to the active site of a second enzyme, E2, via an E1−X−E2 intermediate. The second enzyme E2 then completes its reaction to yield the final product P. The known degree of association between enzyme pairs involved in substrate channeling ranges all the way from covalent attachment to very transient association. In the enzyme carbamoyl phosphate synthase, channeling of ammonia occurs between active sites that are on the same monomer yet separated by many tens of angstroms (*37*). In other examples, the active sites involved in channeling are on different subunits of tightly associated quaternary structures. This is the case in tryptophan synthase (*36*), lumazine synthase/riboflavin synthase (*38*), and the pyruvate dehydrogenase complex (*39*). For most of the proposed channeling pairs among glycolytic enzymes, no stable complex has been isolated, but transient association can be detected using gel filtration (*40*, *41*).

A variety of kinetic methods have been developed to test for substrate channeling. The approach that we use here is the enzyme buffering test (*34*), which has been used most extensively for the study of NADH channeling between glycolytic enzymes (*42*, *43*) and between mitochondrial dehydrogenases and NADH:ubiquinone oxidoreductase complex I (*44*, *45*). In the enzyme buffering method, the activity of E2 is measured in the presence of X and an excess of E1. An expected activity is calculated assuming that only the dissociative mechanism is operating. If the observed activity is higher than expected, then the assumption must be wrong, and the most plausible alternative explanation is the channeling mechanism. In general, the higher the ratio of v_{obs} to v_{calcd}, the stronger the conclusion of substrate channeling. The ratios in this study are similar to the ratios (~10) reported for NADH channeling in the NADH:ubiquinone complex I (*44*), which are among the highest reported using

the enzyme buffering test. The enzyme buffering results for the MerB/Hg/DTT complex are somewhat unusual in that the observed E2 activity is higher than what is expected based on a dissociative mechanism even in the complete absence of excess free enzyme E1 (Table 6). Often, conclusive evidence for substrate channeling does not appear until there is sufficient excess E1 to buffer down the expected amount of free intermediate metabolite X. However, the MerB/Hg/DTT complex is stable enough that the expected amount of free Hg(II) is very low even in the absence of excess MerB.

A prerequisite for the enzyme buffering test is knowledge of the behavior of E2 using free X as a substrate. This is needed in order to calculate the expected activity. This information can be taken from the literature, but it is better to redetermine the kinetic parameters in the same laboratory where the enzyme buffering experiments are done, to control for laboratory specific influences on the kinetic parameters. Many factors influence the activity of MerA, such as the purity of the preparation, the exact gene sequence, the storage conditions, the temperature of the assays, the fraction of the enzyme bound to the flavin cofactor, and the buffer conditions. However, because these factors will influence the control and the enzyme buffering experiments equally, they will not affect the final conclusion of experiments done in tandem.

It is also important that the model for E2 activity corresponds to the conditions and range of X concentrations likely to be encountered in the enzyme buffering test. Over a Hg(II) concentration range of 0−4 μM, we measured a specific v_{max} of 123 min^{-1} and a K_M of 1.0 μM (Figure 6B). This concentration range corresponds to the free Hg(II) expected in the enzyme buffering test (Table 6). Because MerA is a dimeric enzyme with a fairly complicated mechanism (*19*, *26*), this simple Michaelis−Menten model cannot be expected to accurately describe the behavior of MerA outside of this concentration range. This is probably the most important reason that our measurement of the absolute v_{max} (123 min^{-1}) is lower than the absolute v_{max} (1044 min^{-1}) measured in the realm of 100 μM mercuric ion substrate (*26*). Another measurement placed v_{max} of MerA at 340 min^{-1} (*18*), which may be higher than our measurement largely due to the higher temperature used in that study (37 vs 21 °C). The laboratory specific factors mentioned above also certainly contribute to the differences observed between this measurement of the MerA kinetic parameters and the previous measurements. The differences also illustrate the necessity of performing independent measurements of E2 kinetic parameters when doing enzyme buffering experiments.

The enzyme buffering method is subject to several known artifacts relating to enzyme impurity. We have already discussed how E2 (MerA) impurity can be controlled by measuring the kinetic constants in the same laboratory. There are also issues related to E1 (MerB) impurity (*46*). If the E1 preparation is impure, i.e., the true E1 concentration is lower than what is reported, then the calculated free X concentration (second column in Table 6) will be artificially low. This in turn leads to an underestimation of v_{calcd}, which can lead to a false conclusion of substrate channeling. This potential problem is mitigated in our study by the way in which the E1/X (MerB/Hg/DTT) complex is prepared. The MerB/Hg/DTT complex used in enzyme buffering experiments was thoroughly separated from excess mercury and thiols by gel filtration. The only way a mercuric ion can make it to the enzyme buffering assay is as part of a MerB/Hg/DTT complex. This ensures that the E1/X ratio is at least 1:1. The addition of excess free MerB increases the ratio above 1:1. Even if the MerB preparation used were only 50% pure, the final results would not be greatly altered. Still, it should be noted that our MerB preparations appeared at least 95% pure on a Coomassie Blue-stained gel, and this pure band represents a protein population which adopts a single conformation, as judged by NMR spectroscopy.

In enzyme buffering experiments, a relatively large concentration (several micromolar) of E1 is used, whereas only a catalytic amount (nanomolar) of E2 is used. Because of this, minor contaminants in E1 that have enzymatic activity similar to E2 can cause problems. An E1 contaminant that produces false E2 activity will raise the observed activity, but not the expected activity, and can therefore lead to a false conclusion of channeling (*47*). Fortunately, this problem is easily detected by control assays in which E2 is omitted. In this study, no significant MerA-like activity was detected in the absence of MerA.

Other Tests for Channeling. Recently, Geck and Kirsch (*48*) have developed a new test for substrate channeling based on inactivated forms of the E1 enzyme. This test avoids some of the potential problems associated with the need for large amounts of E1 in the enzyme buffering test. Also, the Geck−Kirsch method can disprove the channeling hypothesis, whereas the enzyme buffering test can only disprove the dissociative mechanism and is inconclusive in cases where channeling does not occur. The Geck−Kirsch method requires a variant of E1 that is unable to complete its reaction but interacts with E2 in the same way normal E1 does (assuming such interaction occurs at all). It may be difficult to meet both of these conditions simultaneously in the case of the MerA−MerB pair, because the proposed interaction occurs indirectly through the mercuric ion itself (Figure 8E). There are several catalytically impaired variants of MerB available (*17*), but it is not clear if they bind mercury in the same way or could be expected to interact with MerA in the same way, as wild-type MerB.

Summary. We have shown that simple addition of an organomercurial substrate to MerB in the presence of DTT results in a very stable, reproducible MerB/Hg/DTT complex. The spectra of free MerB and of the MerB/Hg/DTT complex are very similar, showing that the two forms have the same overall fold. The evidence that the complex includes a DTT molecule bound in cyclic fashion includes consideration of 2D $^{1}H-^{15}N$ spectra. In the presence of a racemic mixture of DTT, the resonances of several amide groups appear as sets of closely paired peaks. In the presence of a single optically pure enantiomer of DTT, these resonances appear as single peaks. In the presence of the *meso* isomer of DTT, DTE, these resonances appear as single peaks. These observations are only consistent with a single DTT molecule bound to the mercury atom through both sulfur atoms. EXAFS studies of the MerB/Hg/DTT complex indicate that mercury is coordinated by three sulfurs. The C_β chemical shifts of cysteine residues in the MerB/Hg/DTT complex indicate that the mercury atom is bound to C96. Taken together, the data are consistent with a model for the MerB/Hg/DTT complex in which the mercuric ion is bound by both sulfurs from

DTT and the sulfur of C96. We have used an enzyme buffering test to show that the MerB/Hg/DTT complex can act as a substrate for MerA. We have determined the solution structure of free MerB by NMR (*49*) and are currently determining the solution structure of the MerB/Hg/DTT complex in order to better understand the structure and mechanism of this unique enzyme.

ACKNOWLEDGMENT

We thank Ryan Slackman and Lindsay Hawkins for assistance in the preparation of protein samples. We thank Dr. Anne O. Summers and Keith Pitts for the plasmid containing R831b *merB*. We thank Dr. Richard Meagher for the pNS2 MerA plasmid and for stimulating discussions. We thank Dr. Frank Delaglio, Dr. Bruce Johnson, and Dr. Daniel Garrett for supplying NMR data processing and analysis programs and Dr. Lewis Kay for supplying NMR pulse sequences.

REFERENCES

1. Ditri, P. A., and Ditri, F. M. (1978) Mercury contamination—human tragedy, *Environ. Manage. 2*, 3−16.
2. Morel, F. M. M., Kraepiel, A. M. L., and Amyot, M. (1998) The chemical cycle and bioaccumulation of mercury, *Annu. Rev. Ecol. Syst. 29*, 543−566.
3. Schroeder, W. H., and Munthe, J. (1998) Atmospheric mercury—an overview, *Atmos. Environ. 32*, 809−822.
4. Pak, K. R., and Bartha, R. (1998) Mercury methylation and demethylation in anoxic lake sediments and by strictly anaerobic bacteria, *Appl. Environ. Microbiol. 64*, 1013−1017.
5. Choi, S. C., and Bartha, R. (1994) Environmental factors affecting mercury methylation in estuarine sediments, *Bull. Environ. Contam. Toxicol. 53*, 805−812.
6. Mason, R. P., Reinfelder, J. R., and Morel, F. M. M. (1995) Bioaccumulation of mercury and methylmercury, *Water, Air, Soil Pollut. 80*, 915−921.
7. EPA (1997) *Mercury Study Report to Congress*, EPA-452/R-97-003, U.S. Environmental Protection Agency, Washington, D.C.
8. Mulligan, C. N., Yong, R. N., and Gibbs, B. F. (2001) Remediation technologies for metal-contaminated soils and groundwater: an evaluation, *Eng. Geol. 60*, 193−207.
9. Wagner-Dobler, I., Canstein, H., Li, Y., Timmis, K. N., and Deckwer, W. D. (2000) Removal of mercury from chemical wastewater by microoganisms in technical scale, *Environ. Sci. Technol. 34*, 4628−4634.
10. Rugh, C. L., Wilde, H. D., Stack, N. M., Thompson, D. M., Summers, A. O., and Meagher, R. B. (1996) Mercuric ion reduction and resistance in transgenic *Arabidopsis thaliana* plants expressing a modified bacterial *merA* gene, *Proc. Natl. Acad. Sci. U.S.A. 93*, 3182−3187.
11. Bizily, S. P., Rugh, C. L., and Meagher, R. B. (2000) Phytodetoxification of hazardous organomercurials by genetically engineered plants, *Nat. Biotechnol. 18*, 213−217.
12. Rugh, C. L. (2001) Mercury detoxification with transgenic plants and other biotechnological breakthroughs for phytoremediation, *In Vitro Cell. Dev. Biol.: Plant 37*, 321−325.
13. Meagher, R. B. (2000) Phytoremediation of toxic elemental and organic pollutants, *Curr. Opin. Plant Biol. 3*, 153−162.
14. Summers, A. O. (1986) Organization, expression, and evolution of genes for mercury resistance, *Annu. Rev. Microbiol. 40*, 607−634.
15. Barkay, T., Miller, S. M., and Summers, A. O. (2003) Bacterial mercury resistance from atoms to ecosystems, *FEMS Microbiol. Rev. 27*, 355−384.
16. Begley, T. P., Walts, A. E., and Walsh, C. T. (1986) Mechanistic studies of a protonolytic organomercurial cleaving enzyme-bacterial organomercurial lyase, *Biochemistry 25*, 7192−7200.
17. Pitts, K. E., and Summers, A. O. (2002) The roles of thiols in the bacterial organomercurial lyase (MerB), *Biochemistry 41*, 10287−10296.
18. Moore, M. J., Distefano, M. D., Zydowsky, L. D., Cummings, R. T., and Walsh, C. T. (1990) Organomercurial lyase and mercuric ion reductase- Nature's mercury detoxification catalysts, *Acc. Chem. Res. 23*, 301−308.
19. Miller, S. M., Massey, V., Williams, C. H., Ballou, D. P., and Walsh, C. T. (1991) Communication between the active-sites in dimeric mercuric ion reductase- an alternating sites hypothesis for catalysis, *Biochemistry 30*, 2600−2612.
20. Schiering, N., Kabsch, W., Moore, M. J., Distefano, M. D., Walsh, C. T., and Pai, E. F. (1991) Structure of the detoxification catalyst mercuric ion reductase from *Bacillus sp.* strain RC607, *Nature 352*, 168−172.
21. Moore, M. J., and Walsh, C. T. (1989) Mutagenesis of the N-terminal and C-terminal cysteine pairs of Tn501 mercuric ion reductase- consequences for bacterial detoxification of mercurials, *Biochemistry 28*, 1183−1194.
22. Engst, S., and Miller, S. M. (1999) Alternative routes for entry of HgX_2 into the active site of mercuric ion reductase depend on the nature of the X ligands, *Biochemistry 38*, 3519−3529.
23. Miller, S. M. (1999) Bacterial detoxification of Hg(II) and organomercurials, *Essays Biochem. 34*, 17−30.
24. Ogawa, H. I., Tolle, C. L., and Summers, A. O. (1984) Physical and genetic map of the organomercury resistance (omr) and inorganic mercury resistance (hgr) loci of the IncM plasmid R831B, *Gene 32*, 311−320.
25. Begley, T. P., Walts, A. E., and Walsh, C. T. (1986) Bacterial organomercurial lyase—overproduction, isolation, and characterization, *Biochemistry 25*, 7186−7192.
26. Rinderle, S. J., Booth, J. E., and Williams, J. W. (1983) Mercuric reductase from R-plasmid NR1- characterization and mechanistic study, *Biochemistry 22*, 869−876.
27. Kay, L. E., Keifer, P., and Saarinen, T. (1992) Pure absorption gradient enhanced heteronuclear single quantum correlation spectroscopy with improved sensitivity, *J. Am. Chem. Soc. 114*, 10663−10665.
28. Delaglio, F., Grzesiek, S., Vuister, G. W., Zhu, G., Pfeifer, J., and Bax, A. (1995) NMRPipe—a multidimensional spectral processing system based on Unix pipes, *J. Biomol. NMR 6*, 277−293.
29. Scott, R. A. (2000) X-ray Absorption Spectroscopy, in *Physical Methods in Bioinorganic Chemistry. Spectroscopy and Magnetism* (Que, L., Ed.) pp 465−503, University Science Books, Sausalito, CA.
30. Di Lello, P., Benison, G. C., Omichinski, J. G., and Legault, P. (2004) ^{1}H, ^{15}N, and ^{13}C resonance assignment of the 23 kDa organomercurial lyase MerB in its free and mercury-bound forms. *J. Biomol. NMR*, in press.
31. Utschig, L. M., Wright, J. G., and O'Halloran, T. V. (1993) Biochemical and spectroscopic probes of mercury(II) coordination environments in proteins, *Methods Enzymol. 226*, 71−97.
32. Sharma, D., and Rajarathnam, K. (2000) ^{13}C NMR chemical shifts can predict disulfide bond formation, *J. Biomol. NMR 18*, 165−171.
33. Cheesman, B. V., Arnold, A. P., and Rabenstein, D. L. (1988) Nuclear magnetic resonance studies of the solution chemistry of metal complexes. $Hg(thiol)_3$ complexes and Hg(II)-thiol ligand exchange kinetics, *J. Am. Chem. Soc. 110*, 6359−6364.
34. Spivey, H. O., and Ovadi, J. (1999) Substrate channeling, *Methods 19*, 306−321.
35. Brown, N. L., Camakaris, J., Lee, B. T. O., Williams, T., Morby, A. P., Parkhill, J., and Rouch, D. A. (1991) Bacterial resistances to mercury and copper, *J. Cell. Biochem. 46*, 106−114.
36. Miles, E. W., Rhee, S., and Davies, D. R. (1999) The molecular basis of substrate channeling, *J. Biol. Chem. 274*, 12193−12196.
37. Holden, H. M., Thoden, J. B., and Raushel, F. M. (1998) Carbamoyl phosphate synthetase: a tunnel runs through it, *Curr. Opin. Struct. Biol. 8*, 679−685.
38. Kis, K., and Bacher, A. (1995) Substrate channeling in the lumazine synthase-riboflavin synthase complex of *Bacillus subtilis*, *J. Biol. Chem. 270*, 16788−16795.
39. Wallis, N. G., Allen, M. D., Broadhurst, R. W., Lessard, I. A. D., and Perham, R. N. (1996) Recognition of a surface loop of the lipoyl domain underlies substrate channelling in the pyruvate dehydrogenase multienzyme complex, *J. Mol. Biol. 263*, 463−474.
40. Malhotra, O. P., Prabhakar, P., Sengupta, T., and Kayastha, A. M. (1995) Phosphoglycerate-kinase glyceraldehyde-3-phosphate-dehydrogenase interaction—molecular mass studies, *Eur. J. Biochem. 227*, 556−562.
41. Brooks, S. P. J., and Storey, K. B. (1991) The effect of enzyme-enzyme complexes on the overall glycolytic rate in vivo, *Biochem. Int. 25*, 477−489.
42. Srivastava, D. K., and Bernhard, S. A. (1986) Metabolite transfer via enzyme-enzyme complexes, *Science 234*, 1081−1086.

43. Srivastava, D. K., and Bernhard, S. A. (1984) Direct transfer of reduced nicotinamide adenine-dinucleotide from glyceraldehyde-3-phosphate dehydrogenase to liver alcohol dehydrogenase, *Biochemistry 23*, 4538−4545.
44. Fukushima, T., Decker, R. V., Anderson, W. M., and Spivey, H. O. (1989) Substrate channeling of NADH and binding of dehydrogenases to complex I, *J. Biol. Chem. 264*, 16483−16488.
45. Ushiroyama, T., Fukushima, T., Styre, J. D., and Spivey, H. O. (1992) Substrate channeling of NADH in mitochondrial redox processes, *Curr. Top. Cell. Regul. 33*, 291−307.
46. Gutfreund, H., and Chock, P. B. (1991) Substrate channeling among glycolytic-enzymes—fact or fiction, *J. Theor. Biol. 152*, 117−121.
47. Spivey, H. O. (1991) Evidence of NADH channeling between dehydrogenases, *J. Theor. Biol. 152*, 103−107.
48. Geck, M. K., and Kirsch, J. F. (1999) A novel, definitive test for substrate channeling illustrated with the aspartate aminotransferase-malate dehydrogenase system, *Biochemistry 38*, 8032−8037.
49. Di Lello, P., Benison, G. C., Legault, P., Summers, A. O., and Omichinski, J. G. (2004) NMR structural studies reveal a novel protein fold for MerB, the organomercurial lyase involved in the bacterial mercury resistance system. *Biochemistry 43*, 8322−8332.
50. Ovadi, J. (1991) Physiological significance of metabolic channeling, *J. Theor. Biol. 152*, 1−22.

BI049662H